

Models of $f(R)$ Cosmic Acceleration that Evade Solar-System Tests

Wayne Hu^{1,2} and Ignacy Sawicki^{1,3*}

¹ *Kavli Institute for Cosmological Physics, Enrico Fermi Institute, University of Chicago, Chicago IL 60637*

² *Department of Astronomy & Astrophysics, University of Chicago, Chicago IL 60637*

³ *Department of Physics, University of Chicago, Chicago IL 60637*

(Dated: February 11, 2013)

We study a class of metric-variation $f(R)$ models that accelerates the expansion without a cosmological constant and satisfies both cosmological and solar-system tests in the small-field limit of the parameter space. Solar-system tests *alone* place only weak bounds on these models, since the additional scalar degree of freedom is locked to the high-curvature general-relativistic prediction across more than 25 orders of magnitude in density, out through the solar corona. This agreement requires that the galactic halo be of sufficient extent to maintain the galaxy at high curvature in the presence of the low-curvature cosmological background. If the galactic halo and local environment in $f(R)$ models do not have substantially deeper potentials than expected in Λ CDM, then cosmological field amplitudes $|f_R| \gtrsim 10^{-6}$ will cause the galactic interior to evolve to low curvature during the acceleration epoch. Viability of large-deviation models therefore rests on the structure and evolution of the galactic halo, requiring cosmological simulations of $f(R)$ models, and not directly on solar-system tests. Even small deviations that conservatively satisfy both galactic and solar-system constraints can still be tested by future, percent-level measurements of the linear power spectrum, while they remain undetectable to cosmological-distance measures. Although we illustrate these effects in a specific class of models, the requirements on $f(R)$ are phrased in a nearly model-independent manner.

PACS numbers:

I. INTRODUCTION

Cosmic acceleration, in principle, can arise not from dark energy—a new, exotic form of matter—but rather from a modification of gravity that appears on large scales. The addition of a non-linear function of the Ricci scalar R to the Einstein-Hilbert action has been demonstrated to cause acceleration for a wide variety of $f(R)$ functions [1, 2, 3, 4, 5, 6, 7, 8, 9, 10, 11, 12, 13, 14, 15, 16, 17, 18, 19, 20, 21, 22, 23, 24, 25, 26, 27, 28, 29, 30, 31, 32, 33, 34, 35, 36, 37, 38, 39, 40, 41, 42, 43, 44, 45, 46, 47, 48, 49, 50, 51, 52, 53, 54, 55, 56, 57, 58, 59, 60, 61, 62].

What is less clear in the literature is whether any proposed metric-variation $f(R)$ modification can simultaneously satisfy stringent solar-system bounds on deviations from general relativity as well as accelerate the expansion at late times [63, 64, 65, 66, 67, 68, 69, 70, 71, 72, 73, 74]. Chiba [75] showed that the fundamental difficulty is that $f(R)$ gravity introduces a scalar degree of freedom with the same coupling to matter as gravity that, at the background cosmological density, is extremely light. This light degree of freedom produces a long-range fifth force or, equivalently, a dissociation of the curvature of the space-time from the local density. As a result, the metric around the Sun is predicted to be different than is implied by observations. This problem has been explicitly proven to exist for a wide variety of $f(R)$ models, if the Sun is placed into a background of cosmological density [76, 77].

If high density could be re-associated with high curvature this difficulty would disappear. The scalar degree of freedom would become massive in the high-density solar vicinity and hidden from solar-system tests by the so-called chameleon mechanism [78, 79, 80]. This requires a form for $f(R)$ where the mass squared of the scalar is large and positive at high curvature [61]. Such a condition is also required for agreement with high-redshift cosmological tests from the cosmic microwave background (CMB) [81, 82]. It should be considered as a necessary condition for a successful $f(R)$ model; it is violated in the original inverse-curvature model and many other generalizations (e.g. [83]).

Faulkner *et al.* [80] analyzed a class of models where solar-system tests of gravity could be evaded, but only at the price of reintroducing the cosmological constant as a constant piece of $f(R)$ that drives the cosmic acceleration but is unrelated to local modifications of gravity. Moreover, for these models to satisfy local constraints, all aspects of the cosmology are essentially indistinguishable from general relativity with a cosmological constant.

In this *Paper*, we introduce a class of $f(R)$ models that do not contain a cosmological constant and yet are explicitly designed to satisfy cosmological and solar-system constraints in certain limits of parameter space. We use these models to ask under what circumstances it is possible to significantly modify cosmological predictions and yet evade all local tests of gravity.

We begin in §II by introducing the model class, its effect on the background expansion history and the growth of structure. We show that cosmological tests of the growth of structure can, in principle, provide extremely precise tests of $f(R)$ gravity that rival local constraints

*Electronic address: whu@background.uchicago.edu

and complement them in a very different range in curvature. We then analyze local tests of gravity in §III and show that solar-system tests *alone* are fairly easy to evade, provided gravity behaves similarly to general relativity in the galaxy. However, if cosmological deviations from general relativity are required to be large, the latter condition is satisfied only with extreme and testable changes to the galactic halo. We discuss these results in §IV.

II. $f(R)$ COSMOLOGY

In this section, we discuss the cosmological impact of $f(R)$ models of the acceleration. We begin in §II A by introducing a class of models that accelerate the expansion without a true cosmological constant but nonetheless includes the phenomenology of Λ CDM as a limiting case. We then describe the background equations of motion (§II B) and their representation as an equation for the scalar degree of freedom (§II C). Finally, we calculate the expansion history (§II D) and linear power spectrum (§II E) in our class of $f(R)$ models.

A. Model

We consider a modification to the Einstein-Hilbert action of the form [84]

$$S = \int d^4x \sqrt{-g} \left[\frac{R + f(R)}{2\kappa^2} + \mathcal{L}_m \right], \quad (1)$$

where R is the Ricci scalar, which we will refer to as the curvature, $\kappa^2 \equiv 8\pi G$, and \mathcal{L}_m is the matter Lagrangian. Note that a constant f is simply a cosmological constant. We work in the Jordan frame throughout this paper.

We choose the functional form of $f(R)$ to satisfy certain observationally desirable properties. Firstly, the cosmology should mimic Λ CDM in the high-redshift regime where it is well-tested by the CMB. Secondly, it should accelerate the expansion at low redshift with an expansion history that is close to Λ CDM, but without a true cosmological constant. Thirdly, there should be sufficient degrees of freedom in the parametrization to encompass as broad a range of low-redshift phenomena as is currently observationally acceptable. Finally, for the purposes of constraining small deviations from general relativity with cosmological and solar-system tests, it should include the phenomenology of Λ CDM as a limiting case.

These requirements suggest that we take

$$\begin{aligned} \lim_{R \rightarrow \infty} f(R) &= \text{const.}, \\ \lim_{R \rightarrow 0} f(R) &= 0, \end{aligned} \quad (2)$$

which can be satisfied by a general class of broken power law models

$$f(R) = -m^2 \frac{c_1 (R/m^2)^n}{c_2 (R/m^2)^n + 1}, \quad (3)$$

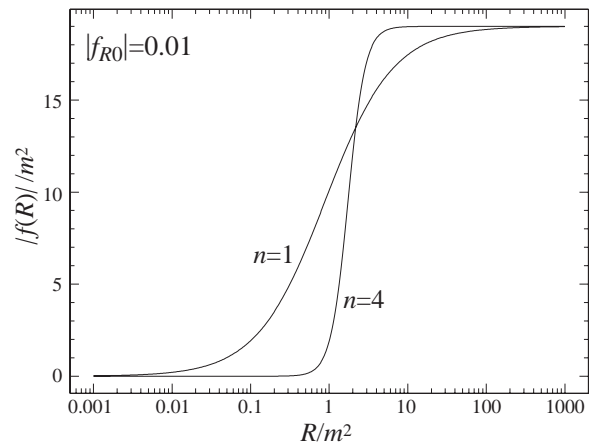


FIG. 1: Functional form of $f(R)$ for $n = 1, 4$, with normalization parameters c_1, c_2 given by $|f_{R0}| = 0.01$ and a matching to Λ CDM densities (see §II D). These functions transition from zero to a constant as R exceeds m^2 . The sharpness of the transition increases with n and its position increases with $|f_{R0}|$. During cosmological expansion, the background only reaches $R/m^2 \sim 40$ for $|f_{R0}| \ll 1$ and so the functional dependence for smaller R/m^2 has no impact on the phenomenology.

with $n > 0$, and for convenience we take the mass scale

$$m^2 \equiv \frac{\kappa^2 \bar{\rho}_0}{3} = (8315 \text{Mpc})^{-2} \left(\frac{\Omega_m h^2}{0.13} \right), \quad (4)$$

where $\bar{\rho}_0 = \bar{\rho}(\ln a = 0)$ is the average density today. c_1 and c_2 are dimensionless parameters. It is useful to note that

$$\frac{\kappa^2 \rho}{m^2} = 1.228 \times 10^{30} \left(\frac{\rho}{1 \text{g cm}^{-3}} \right) \left(\frac{\Omega_m h^2}{0.13} \right)^{-1}. \quad (5)$$

The sign of $f(R)$ is chosen so that its second derivative

$$f_{RR} \equiv \frac{d^2 f(R)}{dR^2} > 0 \quad (6)$$

for $R \gg m^2$, to ensure that, at high density, the solution is stable at high-curvature [61]. This condition also implies that cosmological tests at high redshift remain the same as in general relativity (GR). For example, the physical matter density $\Omega_m h^2$ inferred from the CMB using GR remains valid for the $f(R)$ models. As such, m is a better choice of scale than H_0 since it does not vary for $f(R)$ models in this class. A few examples of the $f(R)$ functions are shown in Fig. 1.

There is no true cosmological constant introduced in this class, unlike in the models of [85]. However, at curvatures high compared with m^2 , $f(R)$ may be expanded as

$$\lim_{m^2/R \rightarrow 0} f(R) \approx -\frac{c_1}{c_2} m^2 + \frac{c_1}{c_2^2} m^2 \left(\frac{m^2}{R} \right)^n. \quad (7)$$

Thus the limiting case of $c_1/c_2^2 \rightarrow 0$ at fixed c_1/c_2 is a cosmological constant in both cosmological and local tests

of gravity, as we shall see. Moreover, at finite c_1/c_2^2 , the curvature freezes into a fixed value and ceases to decline with the matter density, creating a class of models that accelerate in a manner similar to Λ CDM. These models therefore also do not exhibit the problems of “mCDTT” models with the form $f(R) = \mu^4/R$. (Note the sign difference from the original inverse curvature CDTT model [1].) While these models can accelerate the expansion, they evolve in the future into an unstable regime where $1 + f_R < 0$ and also do not contain Λ CDM as a limiting case of the parameter space [82]. Note that $n = 1$ resembles the mCDTT plus a cosmological constant at high curvature. Likewise $n = 2$ resembles the inverse curvature squared model [34] plus a cosmological constant.

B. Background Evolution Equations

Variation of the action (1) with respect to the metric yields the modified Einstein equations

$$G_{\alpha\beta} + f_R R_{\alpha\beta} - \left(\frac{f}{2} - \square f_R\right) g_{\alpha\beta} - \nabla_\alpha \nabla_\beta f_R = \kappa^2 T_{\alpha\beta}, \quad (8)$$

where the field,

$$f_R \equiv \frac{df(R)}{dR}, \quad (9)$$

will play a central role in the analyses below.

Since modifications only appear at low redshift, we take a matter-dominated stress-energy tensor. For the background Friedmann-Robertson-Walker (FRW) metric,

$$R = 12H^2 + 6HH', \quad (10)$$

where $H(\ln a)$ is the Hubble parameter and $' \equiv d/d \ln a$. The modified Einstein equations become the modified Friedmann equation

$$H^2 - f_R(HH' + H^2) + \frac{1}{6}f + H^2 f_{RR} R' = \frac{\kappa^2 \bar{\rho}}{3}. \quad (11)$$

To solve these equations, we re-express them in terms of parameters the values of which vanish in the high-redshift limit where $f(R)$ modifications are negligible

$$\begin{aligned} y_H &\equiv \frac{H^2}{m^2} - a^{-3}, \\ y_R &\equiv \frac{R}{m^2} - 3a^{-3}. \end{aligned} \quad (12)$$

Equations (10) and (11) become a coupled set of ordinary differential equations

$$y'_H = \frac{1}{3}y_R - 4y_H, \quad (13)$$

$$\begin{aligned} y'_R &= 9a^{-3} - \frac{1}{y_H + a^{-3}} \frac{1}{m^2 f_{RR}} \\ &\times \left[y_H - f_R \left(\frac{1}{6}y_R - y_H - \frac{1}{2}a^{-3} \right) + \frac{1}{6} \frac{f}{m^2} \right]. \end{aligned} \quad (14)$$

To complete this system, we take the initial conditions at high redshift to be given by detailed balance of perturbative corrections to $R = \kappa^2 \rho$.

The impact of $f(R)$ on the expansion history can be recast as an effective equation of state for a dark energy model with the same history

$$1 + w_{\text{eff}} = -\frac{1}{3} \frac{y'_H}{y_H}. \quad (15)$$

The two equations (13) and (14) combine in the high curvature limit— $a^{-3} \gg y_H, y_R$ —to form

$$y''_H + [\dots] y'_H + \frac{1}{3m^2 f_{RR} a^{-3}} y_H = \text{driving terms}, \quad (16)$$

where $[\dots]$ contains a time-dependent friction term whose exact nature is not relevant for the qualitative argument and the driving terms involve the matter density. As shown in [61], a critical requirement of the model is that $f_{RR} > 0$ such that Eqn. (16) becomes an oscillator equation with real—not imaginary—mass. For the background, it is convenient to express this as the dimensionless quantity

$$B = \frac{f_{RR}}{1 + f_R} R' \frac{H}{H'}. \quad (17)$$

This oscillator equation and the parameter B have a simple interpretation in terms of the scalar field f_R as we shall now see.

C. Field Equations

The impact of $f(R)$ can be alternatively viewed in terms of the field equation for f_R . The trace of Eqn. (8) can be interpreted as the equation of motion for f_R

$$3\square f_R - R + f_R R - 2f = -\kappa^2 \rho. \quad (18)$$

This equation can be recast in the form

$$\square f_R = \frac{\partial V_{\text{eff}}}{\partial f_R}, \quad (19)$$

with the effective potential

$$\frac{\partial V_{\text{eff}}}{\partial f_R} = \frac{1}{3} (R - f_R R + 2f - \kappa^2 \rho). \quad (20)$$

The effective potential has an extremum at

$$R - R f_R + 2f = \kappa^2 \rho. \quad (21)$$

In the high-curvature regime, where $|f_R| \ll 1$ and $|f/R| \ll 1$, the extremum lies at the general-relativistic expectation of $R = \kappa^2 \rho$. The curvature at the extremum is given by

$$m_{f_R}^2 = \frac{\partial^2 V_{\text{eff}}}{\partial f_R^2} = \frac{1}{3} \left(\frac{1 + f_R}{f_{RR}} - R \right) \quad (22)$$

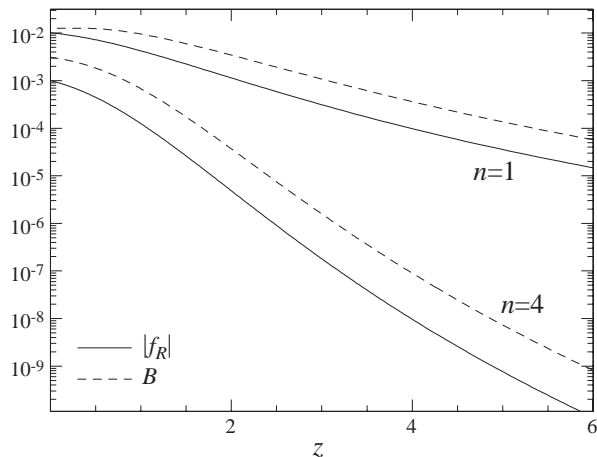


FIG. 2: Cosmological evolution of the scalar field f_R and the Compton wavelength parameter B for models with $n = 1, 4$. Both parameters control observable deviations from general relativity and deviations decline rapidly with redshift as n increases.

and hence the extremum is a minimum for $B > 0$ and a maximum for $B < 0$ in the high-curvature limit with $|f_R|, |f_{RR}R| \ll 1$. Finally the Compton wavelength

$$\lambda_{f_R} \equiv m_{f_R}^{-1}, \quad (23)$$

implies that, in this limit,

$$B^{1/2} \sim \bar{\lambda}_{f_R} H, \quad (24)$$

such that $B^{1/2}$ is essentially the Compton wavelength of f_R at the background curvature in units of the horizon length. The Compton wavelength plays an important role in both cosmological and local tests of $f(R)$ models, as we shall see.

D. Expansion History

We now evaluate the expansion histories for the class of $f(R)$ models in Eqn. (3). First, we would like to narrow the parameter choices to yield expansion histories that are observationally viable, i.e. that deviate from Λ CDM in the effective equation of state (15) by no more than $|1 + w_{\text{eff}}| \lesssim 0.2$ during the acceleration epoch. This equates to choosing a value for the field at the present epoch $f_{R0} \equiv f_R(\ln a = 0) \ll 1$ or, equivalently, $R_0 \gg m^2$. In this case, the approximation of Eqn. (7) applies for the whole past expansion history and the field is always near the minimum of the effective potential

$$R = \kappa^2 \rho - 2f \approx \kappa^2 \rho + 2\frac{c_1}{c_2} m^2, \quad (25)$$

where the $2f$ term is nearly constant and mimics the energy density of a cosmological constant. Thus, to approximate the expansion history of Λ CDM with a cosmological constant $\tilde{\Omega}_\Lambda$ and matter density $\tilde{\Omega}_m$ with respect

to a fiducial critical value, we set

$$\frac{c_1}{c_2} \approx 6 \frac{\tilde{\Omega}_\Lambda}{\tilde{\Omega}_m}, \quad (26)$$

leaving two remaining parameters, n and $c_1/c_2^2 = 6\tilde{\Omega}_\Lambda/c_2\tilde{\Omega}_m$ to control how closely the model mimics Λ CDM. Larger n mimics Λ CDM until later in the expansion history; smaller c_1/c_2^2 mimics it more closely. Note that, since the critical density and Hubble parameter depend on the f_R modification, $\tilde{\Omega}_m$ is only the true value in the limit

$$\lim_{c_1/c_2^2 \rightarrow 0} \tilde{\Omega}_m = \Omega_m, \quad (27)$$

whereas the matter density in physical units remains unchanged $\tilde{\Omega}_m \tilde{H}_0^2 = \Omega_m H_0^2$.

For the flat Λ CDM expansion history

$$R \approx 3m^2 \left(a^{-3} + 4 \frac{\tilde{\Omega}_\Lambda}{\tilde{\Omega}_m} \right), \quad (28)$$

and the field takes on a value of

$$f_R = -n \frac{c_1}{c_2} \left(\frac{m^2}{R} \right)^{n+1}. \quad (29)$$

At the present epoch

$$\begin{aligned} R_0 &\approx m^2 \left(\frac{12}{\tilde{\Omega}_m} - 9 \right), \\ f_{R0} &\approx -n \frac{c_1}{c_2} \left(\frac{12}{\tilde{\Omega}_m} - 9 \right)^{-n-1}, \\ B_0 &\approx \frac{6n(n+1)}{(1+f_{R0})\tilde{\Omega}_m} \frac{c_1}{c_2} \left(\frac{12}{\tilde{\Omega}_m} - 9 \right)^{-n-2}. \end{aligned} \quad (30)$$

In particular, for $\tilde{\Omega}_m = 0.24$ and $\tilde{\Omega}_\Lambda = 0.76$, $R_0 = 41m^2$, $f_{R0} \approx -nc_1/c_2^2/(41)^{n+1}$ and $B_0 \approx -0.61(n+1)f_{R0}$ for $|f_{R0}| \ll 1$. The consequences of cosmological and solar system-tests can be phrased in a nearly model-independent way by quoting the field value f_R . Consequently, we will hereafter parameterize the amplitude c_1/c_2^2 through the cosmological field value today, f_{R0} .

In Fig. 2, we show several examples of the background evolution of f_R . For a fixed present value f_{R0} , a larger n produces a stronger suppression of the field at high redshift and a larger value of B relative to f_R . The steepness of this suppression will play an important role for galactic tests in §III D.

The effective equations of state for these models are shown in Fig. 3. Deviations from a cosmological constant, $w_{\text{eff}} = -1$, are of the same order of magnitude as f_{R0} . This class of models has a phantom effective equation of state, $w_{\text{eff}} < -1$, at high redshift and crosses the phantom divide at a redshift that decreases with increasing n . Note that an effective equation of state that evolves across the phantom divide is a smoking gun for modified gravity acceleration or dark energy with non-canonical degrees of freedom or couplings [86, 87, 88, 89].

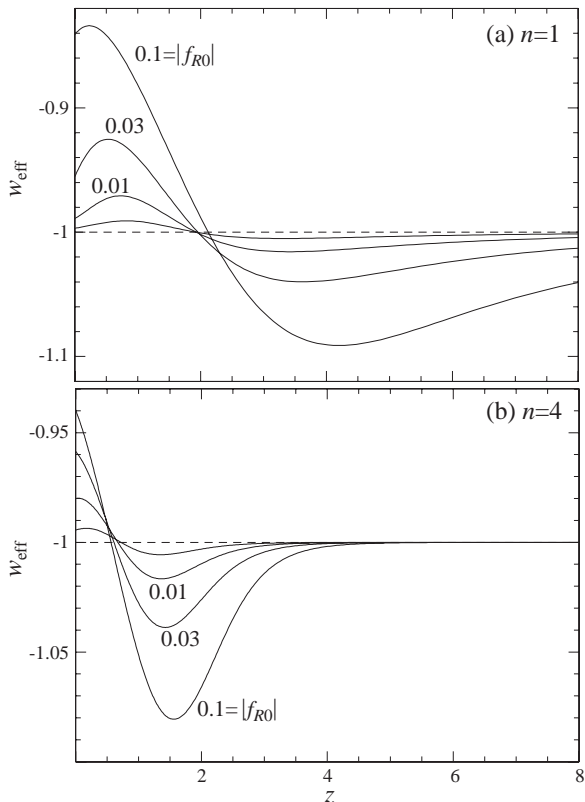


FIG. 3: Evolution of the effective equation of state for $n = 1, 4$ for several values of the cosmological field amplitude today, f_{R0} . The effective equation of state crosses the phantom divide $w_{\text{eff}} = -1$ at a redshift that decreases with increasing n leading potentially to a relatively unique observational signature of these models.

E. Linear Perturbations

Given an expansion history that defines $f_R(\ln a)$ and $B(\ln a)$, the evolution of linear perturbations can be solved using the techniques of [61]. The principal feature of the linear evolution is that once the wavelength of the perturbation becomes smaller than the Compton wavelength in the background

$$\frac{k}{aH} B^{1/2} > 1, \quad (31)$$

strong deviations from the GR growth rate appear. In particular, the space-space Φ and time-time Ψ pieces of the metric fluctuations in the Newtonian (longitudinal) gauge evolve to a ratio

$$-\frac{\Phi}{\Psi} \equiv \gamma = \frac{1}{2}, \quad (32)$$

implying the presence of order-unity deviations from GR.

The consequence of this relative enhancement of the gravitational potential Ψ is an increase in the growth rate of linear density perturbations on scales below the Compton wavelength. If the Compton wavelength is longer

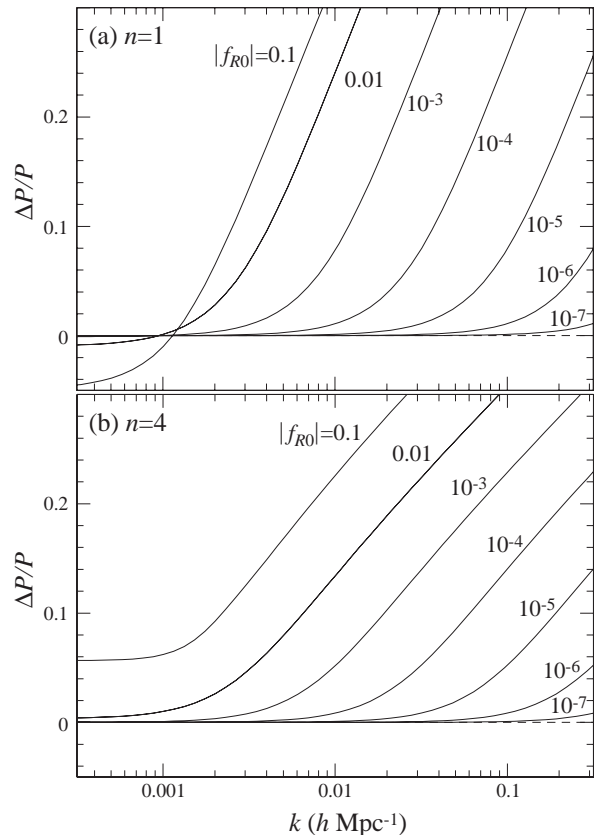


FIG. 4: Fractional change in the matter power spectrum $P(k)$ relative to Λ CDM for a series of the cosmological field amplitude today, f_{R0} , for $n = 1, 4$ models. For scales that are below the cosmological Compton wavelength during the acceleration epoch $k \lesssim (aH)B^{1/2}$ perturbation dynamics transition to the low-curvature regime where $\gamma = 1/2$ and density growth is enhanced. This transition occurs in the linear regime out to field amplitudes of $|f_{R0}| \sim 10^{-6} - 10^{-7}$.

than the non-linear scale of a few Mpc, this transition leads to a strong and potentially observable deviation in the matter power spectrum. Even percent-level deviations in the power spectrum are in principle detectable with future weak-lensing surveys. If the Compton wavelength approaches the horizon, it can substantially alter the CMB power spectrum as well [61].

In Fig. 4, we illustrate this effect for $n = 1$ and $n = 4$ models. Deviations occur in the linear regime down to a field amplitude of $|f_R| \sim 10^{-7}$. For these small field amplitudes, the expansion history and hence distance measures of the acceleration are indistinguishable from a cosmological constant with any conceivable observational probe. Nonetheless, linear structure can provide a precision test of gravity that, we shall see, rivals that of local tests in a substantially different curvature regime.

III. LOCAL TESTS

In this section, we consider local tests of $f(R)$ gravity. We begin in §III A with a general metric around spherically symmetric sources and its relationship to the f_R field. In §III B, we discuss the qualitative behavior of the field solutions and their relationship with the Compton wavelength. We evaluate solar-system constraints in §III C and the requirements they place on the extent and evolution of the galactic halo in §III D.

A. Metric and Field Equations

We take the general spherically symmetric isotropic form for the metric around a source centered at $r = 0$

$$ds^2 = -[1 - 2\mathcal{A}(r) + 2\mathcal{B}(r)]dt^2 + [1 + 2\mathcal{A}(r)](dr^2 + r^2 d\Omega), \quad (33)$$

where we assume that $|\mathcal{A}(r)| \ll 1$ and $|\mathcal{B}(r)| \ll 1$ near the source, such that the metric is nearly Minkowski. In the GR limit, $\mathcal{B}(r) \rightarrow 0$; limits on \mathcal{B} in the solar system provide the strongest tests of modification to gravity of the type considered here.

By definition of the Ricci tensor, the sources of the metric potentials \mathcal{A} and \mathcal{B} are given by

$$\nabla^2(\mathcal{A} + \mathcal{B}) = -\frac{1}{2}R, \quad (34)$$

$$\nabla^2\mathcal{B} = -\frac{1}{2}(R^0_0 + R/2). \quad (35)$$

Note that a low-curvature $R \ll \kappa^2\rho$ solution may be accommodated by $\mathcal{B} \approx -\mathcal{A}$.

To relate the time-time component of the Ricci tensor to $f(R)$, let us take the time-time component of the field equation (8)

$$(1 + f_R)R^0_0 - \frac{1}{2}(R + f) + \square f_R + \partial_t^2 f_R = -\kappa^2\rho. \quad (36)$$

Under the assumption of a static solution, we can combine this equation with the trace equation (18) to obtain

$$R^0_0 = \frac{-2\kappa^2\rho + \frac{1}{2}R - \frac{1}{2}f + f_R R}{3(1 + f_R)}. \quad (37)$$

Even in a low-curvature solution where $R \ll \kappa^2\rho$, $R^0_0 = \mathcal{O}(\kappa^2\rho)$.

Eqn. (35) then becomes

$$\nabla^2\mathcal{B} = -\frac{1}{4} \left(\frac{-4\kappa^2\rho + 4R + 5f_R R - f}{3(1 + f_R)} \right), \quad (38)$$

where $f(R)$ is given by the solution to the trace equation (18) in the static limit

$$3\nabla^2 f_R - R + f_R R - 2f = -\kappa^2\rho. \quad (39)$$

As an aside, choosing models for which $B > 0$ in §II A, not only results in the existence in the expansion history of a stable matter-dominated era, but ensures that the models do not exhibit the related instability for stellar-type objects [90, 91]. Small, time-dependent perturbations to a high-curvature solution of Eqn. (39) have positive mass squared and do not grow in this class of $f(R)$.

In the limit that $|f_R| \ll 1$ and $|f/R| \ll 1$, valid for all sources that we shall consider,

$$\nabla^2\mathcal{A} \approx -\frac{1}{2}\kappa^2\rho + \frac{1}{6}(\kappa^2\rho - R), \quad (40)$$

$$\nabla^2\mathcal{B} \approx \frac{1}{3}(\kappa^2\rho - R). \quad (41)$$

As expected, the source of \mathcal{B} is the deviation of the curvature R from the GR value of $\kappa^2\rho$. Moreover, in the same limit, equation (39) for f_R becomes

$$\nabla^2 f_R \approx \frac{1}{3}(R - \kappa^2\rho). \quad (42)$$

A solution for f_R therefore gives \mathcal{B} up to constants of integration

$$\mathcal{B}(r) = -f_R(r) + a_1 + \frac{a_2}{r}. \quad (43)$$

Since \mathcal{B} must remain finite at $r = 0$, $a_2 = 0$. Let us assume that at sufficiently large radii $f_R(r) \rightarrow f_{R\infty}$ and $\mathcal{B} \rightarrow 0$ then

$$\mathcal{B}(r) = -[f_R(r) - f_{R\infty}] \equiv -\Delta f_R(r). \quad (44)$$

For radii beyond which the source $\kappa^2\rho - R$ becomes negligible $\mathcal{B}(r) \propto 1/r$. It is convenient to then define an effective enclosed mass

$$M_{\text{eff}} = 4\pi \int (\rho - R/\kappa^2)r^2 dr, \quad (45)$$

such that

$$\mathcal{B}(r) = -\Delta f_R(r) \rightarrow \frac{2GM_{\text{eff}}}{3r}. \quad (46)$$

Note that this is an implicit solution, since $R(f_R)$. Nevertheless, we shall see in the next section that it sheds light on the behavior of explicit solutions.

Finally, the deviation from the general-relativistic metric is given by

$$\gamma - 1 \equiv \frac{\mathcal{B}}{\mathcal{A} - \mathcal{B}} \rightarrow -\frac{2M_{\text{eff}}}{3M_{\text{tot}} + M_{\text{eff}}}, \quad (47)$$

where M_{tot} is the total mass of the system. The two limiting cases are $M_{\text{eff}} \ll M_{\text{tot}}$ for which $\gamma - 1 = -2M_{\text{eff}}/3M_{\text{tot}}$ and $M_{\text{eff}} = M_{\text{tot}}$ for which $\gamma - 1 = -1/2$. These solutions correspond to high curvature, $R \approx \kappa^2\rho$, and low curvature, $R \ll \kappa^2\rho$ [76, 77] respectively.

B. Compton and Thin-Shell Conditions

Before examining explicit solutions for $f_R(r)$ given $\rho(r)$, we show how the nature of the solutions is tied to the Compton wavelength of the field and exhibits the so-called chameleon mechanism [78] for hiding scalar degrees of freedom in high-density regions [79, 80].

An examination of Eqn. (39) shows that there are two types of *local* solutions to the field equations distinguished by a comparison of the Compton wavelength of the field f_R

$$\lambda_{f_R} \equiv m_{f_R}^{-1} \approx \sqrt{3f_{RR}}, \quad (48)$$

to the density structure of the source.

Let us again assume that $|f_R| \ll 1$ and $|f/R| \ll 1$ so that the field equation is well approximated by Eqn. (42). The first class of solutions to this equation has high curvature $R \approx \kappa^2 \rho$ and small field gradients $\nabla^2 f_R \ll \kappa^2 \rho$. The second class of solutions has low curvature $R \ll \kappa^2 \rho$ and large field gradients $\nabla^2 f_R \approx -\kappa^2 \rho/3$.

A *sufficient* condition for the high-curvature solution is that field gradients can be ignored at all radii when compared with the density source. A *necessary* or consistency condition is that field gradients implied by the high-curvature solution $f(R = \kappa^2 \rho)$ can be ignored compared with local density gradients. More specifically

$$f_{RR} \Big|_{R=\kappa^2 \rho} \partial_i^2 \rho \ll \rho, \quad f_{RR}^{1/2} \Big|_{R=\kappa^2 \rho} \partial_i \rho \ll \rho, \quad (49)$$

i.e. that the density changes on scales that are much longer than the Compton wavelength. Equivalently, a mass source induces changes in the field with a Yukawa profile of $e^{-m_{f_R} r}/r$ which are highly suppressed on scales larger than the Compton wavelength. We call this condition the Compton condition.

If the Compton condition is satisfied at all radii, then the high-curvature solution is also valid at all radii and deviations from GR will be highly suppressed. If this condition is violated beyond some outer radius, then a portion of the exterior must be at low curvature $R \ll \kappa^2 \rho$. Moreover, since Birkhoff's theorem does not apply, the exterior low-curvature solution can penetrate into the region where the Compton condition (49) is locally satisfied. The interior solution then depends on the exterior conditions. We have seen in §II E that linear cosmological perturbations are in the low-curvature regime on scales smaller than the cosmological Compton wavelength and so the Compton criteria must be violated far in the exterior if $|f_{R0}| \gtrsim 10^{-7}$. We will return to this point in §III D.

To quantify these considerations, note that the maximal change in f_R from the interior to the exterior is imposed by the low-curvature assumption $R \ll \kappa^2 \rho$ or $M_{\text{eff}} = M_{\text{tot}}$

$$\Delta f_R(r) \leq \frac{2}{3} \Phi_M(r), \quad (50)$$

where $\Phi_M(r)$ is the Newtonian potential profile of the source, i.e. $\Phi_M \approx GM_{\text{tot}}/r$ exterior to the dominant mass. This condition sets an upper limit on the difference between the interior and exterior field values for a static solution.

If the thin-shell condition is satisfied and $|\Delta f_R(r)| \ll \Phi_M(r)$, then $M \gg M_{\text{eff}}$ and somewhere in the interior there must exist a high-curvature region where $R \rightarrow \kappa^2 \rho$. To estimate where this occurs consider a local version of Eqn. (50)

$$\Delta f_R \lesssim \kappa^2 (\rho - \rho_\infty) r^2. \quad (51)$$

From the outside in, when this condition is first satisfied, there is enough source to make the transition between the interior and exterior field values. Once this is satisfied, it remains satisfied in the interior as long as further changes in f_R are much smaller than the initial jump. In other words, the exterior field is only generated by the ‘‘thin shell’’ of mass M_{eff} that lies outside of this transition. We will call this the thin-shell criterion and such a solution is known in the literature as a chameleon solution.

The thin-shell criterion is related to the low-curvature linearization condition of [77] Eqn. (13). There, a solution for the curvature is found by linearizing Eqn. (39) around its background value. Requiring that the value of the perturbation be smaller than that of the background curvature, results in exactly the opposite of Eqn. (50)

$$|f_{R\infty}| \gtrsim \frac{2}{3} \Phi_M(r). \quad (52)$$

Therefore, the linearization procedure is not valid for exactly those sets of parameters for which the thin-shell condition is satisfied: high-curvature solutions are necessarily non-linear. When the linearization is valid, the solution is low-curvature everywhere leading to large deviations from GR in the interior.

The thin-shell criterion (51) is also related to but stronger than the local Compton condition

$$f_{RR} < r_\rho^2, \quad (53)$$

where r_ρ is the distance over which the density field changes. Converting derivatives to finite differences $f_{RR} \approx \delta f_R / \delta R$

$$\delta f_R \lesssim \delta R r_\rho^2 \approx \kappa^2 \delta \rho r_\rho^2. \quad (54)$$

The difference between the two conditions is that the Compton condition involves the small change in the field δf_R at high curvature, whereas the thin shell criterion involves the potentially larger change in the field Δf_R from the high- to low-curvature regimes. If there is no transition to low curvature in the exterior then these conditions are the same.

The thin-shell condition implies that the field does not always sit at the local potential minimum $R \approx \kappa^2 \rho$. Nonetheless, the field does choose the energetically favorable configuration. The field f_R will not lie at the

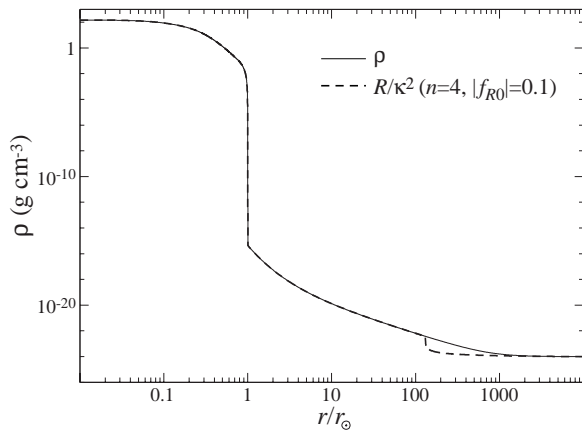


FIG. 5: Density profile in the solar interior and vicinity (solid curve). Under general relativity (GR), the curvature R would track the density profile. For the $f(R)$ model with $n = 4$, cosmological field amplitude $|f_{R0}| = 0.1$ and a galactic field amplitude that minimizes the scalar potential, the curvature tracks the GR or high-curvature limit out to the edge of the solar corona at about 1AU (dashed line).

potential minimum in the interior region if the energy cost for introducing a field gradient between the interior and exterior is too high. The potential energy density cost for not lying at the potential minimum is

$$\Delta V \sim \frac{\kappa^2}{3} \rho |\Delta f_R|, \quad (55)$$

where Δf_R is the difference between potential minimum and the exterior solution. Compare this with the gradient energy density gain from not introducing a profile in the field

$$\Delta E \sim \frac{1}{2} \frac{|\Delta f_R|^2}{r^2}. \quad (56)$$

The potential energy cost outweighs the gain if

$$|\Delta f_R| \lesssim \kappa^2 \rho r^2, \quad (57)$$

which is the thin-shell condition.

C. Solar System to Galaxy

We now consider explicit solutions of the field equation (39), given the density profile $\rho(r)$, in the solar vicinity. In this section, we will assume that the galaxy has sufficient mass and extent to bring the field to the potential minimum of Eqn. (29) in the outskirts of the solar system. In the next section, we will discuss the requirement this assumption places on the structure and evolution of the galactic halo.

Specifically, we set the boundary condition $f_{R\infty} = f_{Rg}$ where

$$f_{Rg} = f_R(R = \kappa^2 \rho_g). \quad (58)$$

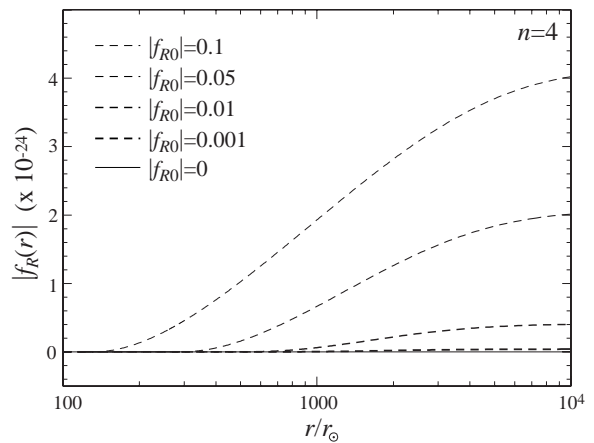


FIG. 6: Solar solution for $f_R(r)$ with $n = 4$ for a series of cosmological field amplitudes f_{R0} with a galactic field that minimizes the potential. The field smoothly transitions from the $f_R \sim 0$ interior value to the galactic values once the thin-shell criterion is violated.

Here, ρ_g is the average galactic density in the solar vicinity. Under this assumption, the galactic field value is related to the cosmological one as

$$\left(\frac{f_{Rg}}{f_{R0}}\right)^{\frac{1}{n+1}} = 8.14 \times 10^{-7} \frac{R_0}{m^2} \frac{\Omega_m h^2}{0.13} \left(\frac{\rho_g}{10^{-24} \text{g cm}^{-3}}\right)^{-1}. \quad (59)$$

For the density profile in the solar vicinity we take the helioseismological model of [92] for the solar interior, the chromosphere model of [93] and the corona model of [94] for the surrounding region. We add to these density profiles a constant galactic density of $\rho_g = 10^{-24} \text{g cm}^{-3}$. This profile is shown in Fig. 5 (solid curve).

We solve the field equation (39) as a boundary-value problem using a relaxation algorithm. The source-free ($\rho = 0$) field equation has exponentially growing and decaying Yukawa homogeneous solutions $\exp(\pm m_{f_R} r)/r$. Initial-value integrators have numerical errors that would stimulate the positive exponential, whereas relaxation methods avoid this problem by enforcing the outer boundary at every step. We show an example solution in Fig. 5 (dashed curve) for $n = 4$ and $|f_{R0}| = 0.1$.

A solution is found on an interval, by requiring that the field f_R minimize the potential (20) at two chosen radii: one far away from the Sun and its corona, the other—inside the solar density distribution. We place the outer boundary at $r = 10^6 r_\odot$, where the density distribution is entirely dominated by the constant galactic-density component. The solutions are robust to increasing the radius of this boundary.

For the inner boundary, we take the starting point as approximately 1000 Compton wavelengths from the transition to low curvature; the Compton condition is well satisfied there. Interior to this point, the solution is more efficiently obtained by a perturbative solution around the high-curvature solution of $R^{(0)} = \kappa^2 \rho$. The first-order

correction to this solution is $R = R^{(0)} + R^{(1)}$ with

$$R^{(1)} = (3\nabla^2 f_R + f_R R - 2f) \Big|_{R=R^{(0)}}. \quad (60)$$

With this correction to R , the first-order correction to f_R can be obtained using initial-value-problem methods. This series can be iterated to arbitrary order and is strongly convergent when the Compton condition is satisfied. In fact, at our chosen starting point, the zeroth order solution typically suffices. We have also checked that for cases where the Compton condition is everywhere satisfied, the numerical solution matches the perturbative solution. Finally, we stop the relaxation code when the solution satisfies the trace equation (39) to at least 10^{-6} accuracy.

Let us now relate the numerical solutions shown in Fig. 6 to the qualitative analysis of the previous section. First, consider the Compton condition. The Compton wavelength at $R = \kappa^2 \rho$ is

$$\begin{aligned} \lambda_{f_R} &= (10.6 \text{ pc}) (8.14 \times 10^{-7})^{(n-1)/2} \\ &\times [(n+1)|f_{R0}|]^{1/2} \left(\frac{R_0 \Omega_m h^2}{m^2 \cdot 0.13} \right)^{(n+1)/2} \\ &\times \left(\frac{\rho}{10^{-24} \text{ g cm}^{-3}} \right)^{-(n+2)/2}. \end{aligned} \quad (61)$$

For example, for $n = 4$ and the fiducial cosmology

$$\lambda_{f_R} \approx (8300 r_\odot) |f_{R0}|^{1/2} \left(\frac{\rho}{10^{-24} \text{ g cm}^{-3}} \right)^{-3}, \quad (62)$$

so that the Compton condition is satisfied for the whole solar profile for $|f_{R0}| \lesssim 10^{-2}$. Note that, even at the base of the corona where the density is $\rho \approx 10^{-15} \text{ g cm}^{-3}$, the Compton wavelength is $\sim 10^{-23} |f_{R0}|^{1/2} r_\odot$. Thus, in spite of the steep density gradient at the edge of the Sun, the Compton condition is well satisfied, allowing the solution in Fig. 5 to follow the high-curvature solution $R = \kappa^2 \rho$ closely through the transition.

On the other hand, the thin-shell criterion is satisfied in the solar corona up to $|f_{R0}| \lesssim 10^{-1}$. Thus for $n = 4$, we expect order-unity cosmological fields to be achievable with the entire solar interior including the edge and chromosphere in the high-curvature regime.

The numerical solutions shown in Fig. 6 verify the qualitative behavior described in the previous section. For $|f_{R0}| \lesssim 10^{-2}$, the deviations from the high-curvature $R = \kappa^2 \rho$ limit are fractionally small since the Compton condition is everywhere satisfied. For $|f_{R0}| \lesssim 10^{-1}$, the break to low curvature occurs in the corona. This break occurs gradually in the field profile $f_R(r)$ but rapidly in the curvature (see Fig. 7). At small field values, a small change in f_R represents a large change in the curvature. M_{eff} is approximately just the mass between this transition and the point at which the galactic density exceeds the corona. Outside of this transition, the exterior field relaxes to the galactic value as $|\Delta f_R| \propto e^{-m f_R r} / r$. In

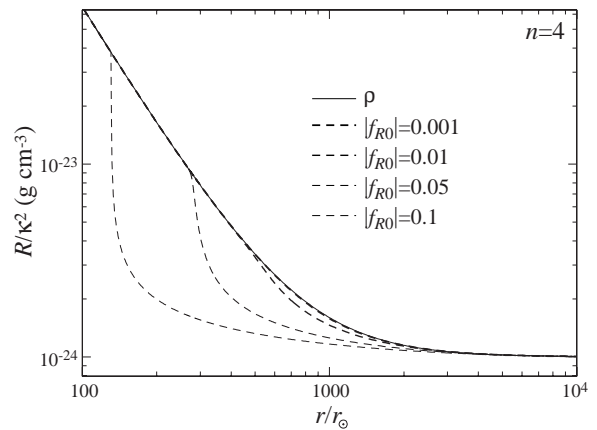


FIG. 7: Solar solution for the curvature R for the $n = 4$ model and a series of cosmological field amplitudes f_{R0} with a galactic field that minimizes the potential. The solution abruptly transitions from the high-curvature $R \approx \kappa^2 \rho$ to the low-curvature regime once the thin-shell criterion is violated.

these examples, the Compton wavelength in the galaxy is of order $10^3 - 10^4 r_\odot$ and the mass term further suppresses the deviations from GR.

In Fig. 8 we show $|\gamma - 1|$ for the same $n = 4$ models. The deviations peak at $\sim 10^{-15}$. Such deviations easily pass the stringent solar system tests of gravity from the Cassini mission [95]

$$|\gamma - 1| < 2.3 \times 10^{-5} \quad (63)$$

under the assumption that the galactic field f_{Rg} is given by the potential minimum.

Models that saturate this observational bound have a sufficiently large $|f_{Rg}|$ that the thin-shell criterion is first satisfied at the edge of the Sun, where the fractional enclosed mass becomes $2M_{\text{eff}}/3M_{\text{tot}} \approx 10^{-5}$ (see Eqn. 47). For a given f_{R0} , this can be achieved by lowering n . In such models, the additional contribution to the effective mass outside of the photosphere is negligible and the field solution obeys Eqn. (46). The exterior solution therefore becomes

$$\Delta f_R(r) \approx (\gamma - 1) \Phi_M(r) \approx (\gamma - 1) \frac{GM_\odot}{r}, \quad (64)$$

since the Compton wavelength in the exterior implied by Eqn. (61) is much larger than the solar system.

Given that

$$\frac{GM_\odot}{r_\odot} = 2.12 \times 10^{-6}, \quad (65)$$

the solar-system constraints can be simply stated as

$$|\Delta f_R(r_\odot)| \approx |f_{Rg}| < 4.9 \times 10^{-11}. \quad (66)$$

Note that this bound is independent of the form of $f(R)$ and the assumption that f_{Rg} is given by the minimum of the effective potential. The model dependence

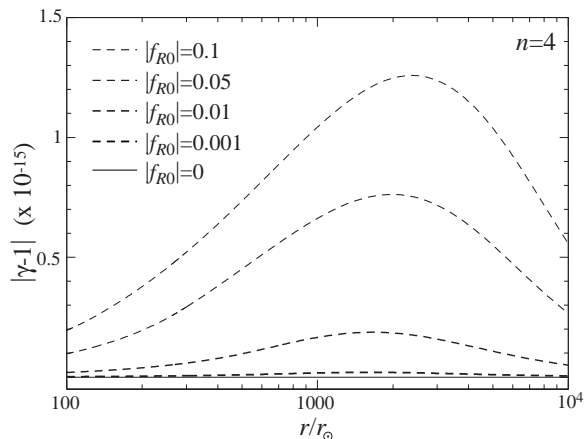


FIG. 8: Metric deviation parameter $|\gamma - 1|$ for $n = 4$ models and a series of cosmological field amplitudes f_{R0} with a galactic field that minimizes the potential. These deviations are unobservably small for the whole range of amplitudes.

comes from the implications for the cosmological field value f_{R0} . Using Eqn. (59) at a galactic density of $\rho_g = 10^{-24} \text{ g cm}^{-3}$, we can translate this into a bound on the amplitude of the cosmological field

$$|f_{R0}| < 74 (1.23 \times 10^6)^{n-1} \left[\frac{R_0 \Omega_m h^2}{m^2 0.13} \right]^{-(n+1)}. \quad (67)$$

As shown in Fig. 9 this is a fairly weak constraint. For $n > 1$ it allows order unity cosmological deviations from GR. Note that the models of [80] are equivalent to a continuation of the approximate form of our model in Eqn. (7) but with $n < 0$. Solar system constraints on cosmological amplitudes are significantly stronger in that class. Finally, although a detailed calculation is beyond the scope of this work, laboratory constraints on fifth forces are also weak under the same assumptions given the much larger effective densities involved [78].

D. Galaxy to Cosmology

The cosmological bound Eqn. (67) from the solar-system constraint Eqn. (66) is robust but weak. A related but potentially more powerful constraint comes from the transition between the high curvature of the galaxy and the desired cosmological curvature. Indeed, the implicit assumption in applying the solar-system constraint to the cosmology is that the galaxy itself is in the high-curvature regime with respect to its own density profile.

The validity of this assumption depends on both the structure of the galactic halo and its evolution during the acceleration epoch. Large $|f_{R0}|$ requires that either the galactic gravitational potential is substantially deeper than in Λ CDM or that it has not yet reached its equilibrium value.

From the linear theory analysis in §II E, we know that the Compton condition is violated for linear perturba-

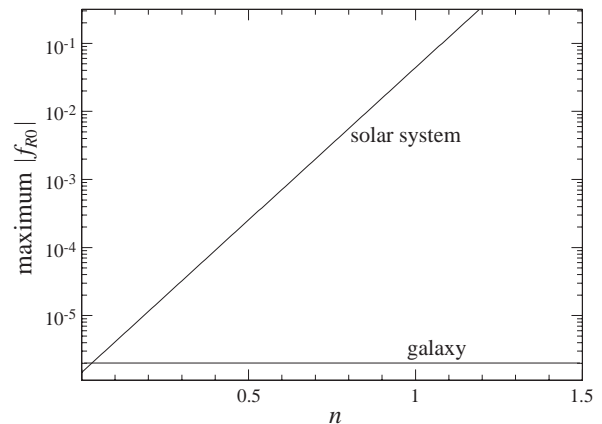


FIG. 9: Maximum cosmological field $|f_{R0}|$ allowed by the solar system constraint alone (top curve) under the assumption that the galactic field remains at the potential minimum at the present epoch. Models with $|f_{R0}| \gtrsim 10^{-6}$ (bottom curve) have galactic fields $|f_{Rg}|$ that evolve to higher values during the acceleration epoch, potentially enabling substantially stronger constraints with structure formation simulations.

tions if $|f_{R0}| \gtrsim 10^{-7}$. Hence, at the outskirts of the galactic halo where the density profile joins onto the large-scale structure of the universe, there must be a transition from high to low curvature. As we have seen in §III B, the low-curvature cosmological field will eventually penetrate into the galaxy unless

$$|\Delta f_R(r)| \equiv |f_{Rg} - f_{R0}| \approx |f_{R0}| \lesssim \frac{2}{3} \Phi_g, \quad (68)$$

where Φ_g is the Newtonian potential of the galaxy. For definiteness, let us consider the NFW density profile

$$\rho_g(r) = \frac{M_g}{4\pi r(r+r_s)^2}, \quad (69)$$

where M_g is the galactic mass contained within $5.3r_s$ and r_s is the scale radius of the dark-matter halo. This density profile has a Newtonian potential of

$$\Phi_g = \frac{GM_g}{r} \ln(1+r/r_s), \quad (70)$$

and a maximum rotation-curve velocity of

$$v_{\max} = 0.46 \left(\frac{GM_g}{r_s} \right)^{1/2} \quad (71)$$

at $2.16r_s$. Taking the thin-shell criterion to be satisfied at $r \approx r_s$, such that the interior is in the high-curvature regime, leads to an upper limit on $|f_{R0}|$ for a static solution of

$$|f_{R0}| \lesssim 2 \times 10^{-6} \left(\frac{v_{\max}}{300 \text{ km/s}} \right)^2. \quad (72)$$

For higher cosmological values of the field $|f_{R0}|$, the galaxy will relax over time to the low-curvature solution to minimize the cost of field gradients. Note that

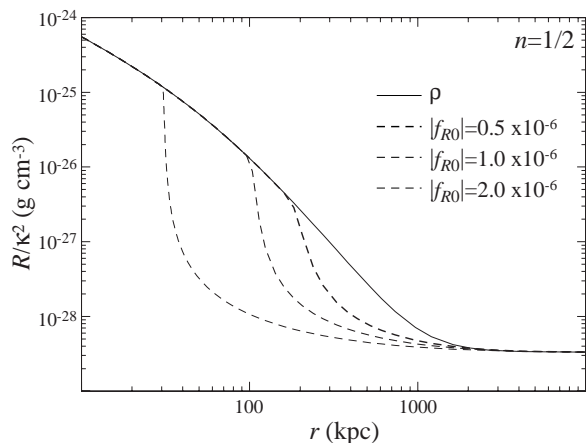


FIG. 10: A galactic solution for the scalar curvature R for $n = 1/2$ with an NFW density profile (69) and conservative parameters $r_s = 75$ kpc and $v_{\max} = 300$ km s $^{-1}$. For $|f_{R0}| \gtrsim 2 \times 10^{-6}$, no *static* solution can be found which has high curvature, $R \approx \kappa^2 \rho$, inside the halo. As in the solar case, once the thin-shell criterion is violated the solution abruptly transitions to low curvature and matches onto the cosmological value of f_{R0} outside the halo.

even a value of $|f_{R0}| = 10^{-6}$ provides potentially observable modifications in the linear regime since gravity at the juncture is still modified by order unity (see Fig. 4). We have verified through the numerical techniques of the previous section that the constraint in Eqn. (72) is nearly independent of the functional form of $f(R)$. In Fig. 10, we show an example solution. Here we err on the conservative side by taking $v_{\max} = 300$ km s $^{-1}$ and $r_s = 75$ kpc to reflect a somewhat more massive and extended halo by a factor of a few than expected in Λ CDM for our galaxy (c.f. [96], Fig. 7). Empirical data exists only out to ~ 20 kpc where the rotational velocity reaches $v \approx 230$ km s $^{-1}$.

Unfortunately, the bound in Eqn. (72) is suggestive but not definitive. A cosmological simulation will be required to determine how haloes of galactic size, which are embedded in a group-sized dark-matter halo, which itself is part of the quasi-linear large-scale structure of the universe, evolve during the acceleration epoch. The density profiles of the structures in which the galaxy is embedded can further shield the galactic interior from the low-curvature solution. Furthermore, the cosmological background itself was at high curvature at $z \gg 1$. For $n \gg 1$, the condition that the background $|f_R| \lesssim 10^{-6}$ is well satisfied for $z \gg 1$ even for f_{R0} approaching unity. For example if $n = 4$, the cosmological field drops by 10^3 by $z = 2$ (see Fig. 2). Therefore when the galactic halo formed both its interior and exterior were at high curvature. The local curvature would then follow the local density $R \approx \kappa^2 \rho$ closely everywhere.

Only during the recent acceleration epoch is the thin-shell criterion for the galaxy violated at $|f_{R0}| \gtrsim 10^{-6}$. The low curvature, high field values of the background

will then begin to propagate into the interior of the galactic halo in a manner that requires a simulation of the process. The static, thin-shell bound for the galaxy given by Eqn. (72) is therefore overly restrictive but suggests that cosmological simulations should enable much more stringent bounds on $f(R)$ models than solar-system test alone.

IV. DISCUSSION

We have introduced a class of $f(R)$ models that accelerate the expansion without a cosmological constant. Its parameters allow the gravitational phenomenology exhibited in cosmological, galactic and solar-system tests to span the range between infinitesimal and order-unity deviations from general relativity with a cosmological constant.

In these models, unlike the original model of [1] and related generalizations, the general-relativistic or high-curvature value for the Ricci scalar $R \approx \kappa^2 \rho$ is the solution that minimizes the potential for the scalar degree of freedom $f_R = df(R)/dR$. This feature is critical for both cosmological and solar-system tests.

Solar-system tests of $f(R)$ gravity *alone* place only weak bounds on these models, despite a strong and nearly model-independent limit on the f_R field amplitude in the galaxy of $|f_{Rg}| < 5 \times 10^{-11}$. Indeed, we show that for a range of models that include cosmological fields of order unity $|f_{R0}| \lesssim 1$, the field deviates from the high-curvature regime only for a brief interval in the solar corona. Likewise, deviations from general relativity in the metric are generated by the mass in this interval and so are unobservably small. This is strikingly different from constraints that would arise if one embeds the Sun directly into a medium at the cosmological density $|f_{R0}| < 5 \times 10^{-11}$.

Without further constraints on the size and evolution of the galactic halo, solar-system tests may be evaded relatively easily. This is because of the assumed strong density scaling of the field amplitude at the potential minimum. However, though the galactic field begins at high redshift at its potential minimum, it will only remain there if the galaxy is sufficiently massive to protect it against the cosmological exterior which is evolving to low curvature at $z < 1$.

An order of magnitude estimate, based on the extrapolation of rotation-curve measurements and the assumption that the galactic halo does not differ substantially from Λ CDM expectations in the outskirts, suggests that an isolated galaxy that is otherwise like our own will only remain stably at high curvature if the cosmological field is $|f_{R0}| \lesssim 10^{-6}$. Despite the fact that the high-curvature solution still minimizes the potential energy of the field, the gradient energy implied by the field profile from the galactic interior to exterior is too high. This estimate is also nearly independent of the functional form of $f(R)$ and improvements in the solar-system constraint. Turn-

ing this estimate into a firm constraint on models will require cosmological simulations of $f(R)$ acceleration to examine how far into the solar system the exterior low-curvature field values can penetrate by the present epoch in the local environment of our galactic halo.

Distance-based measurements of the expansion history will be limited to testing $|f_{R0}| \gtrsim 10^{-3} - 10^{-2}$ for the foreseeable future, since the field amplitude determines the deviations in the effective equation of state to be of comparable size. Nonetheless, future, percent-level constraints on the matter power spectrum in the linear regime offer potentially even stronger tests of $f(R)$ models than solar or galactic constraints, in principle down to amplitudes of $|f_{R0}| \sim 10^{-7}$. This sensitivity is due to the large Compton scale in the background across which perturbations make the transition from low to high curvature and exhibit order-unity deviations from general

relativity. Cosmological simulations are also required to determine how these signatures can be disentangled from the non-linear evolution of structure.

Acknowledgments: We thank S. Basu, S. Carroll, S. DeDeo, A. Erickcek, M. Kamionkowski, D. Kapner, D. Psaltis, B. Robertson, M. Seifert, T. Smith, A. Upadhye, B. Wald and A. Weltman for useful conversations. This work was supported by the U.S. Dept. of Energy contract DE-FG02-90ER-40560. IS and WH are additionally supported by the David and Lucile Packard Foundation and by the KICP under NSF PHY-0114422. IS thanks for the hospitality of the California Institute of Technology where a part of this work was carried out.

-
- [1] S. M. Carroll, V. Duvvuri, M. Trodden, and M. S. Turner, Phys. Rev. **D70**, 043528 (2004), astro-ph/0306438.
 - [2] S. Nojiri and S. D. Odintsov, Int. J. Geom. Meth. Mod. Phys. **4**, 115 (2007), hep-th/0601213.
 - [3] S. Capozziello, Int. J. Mod. Phys. **D11**, 483 (2002), gr-qc/0201033.
 - [4] S. Capozziello, S. Carloni, and A. Troisi (2003), astro-ph/0303041.
 - [5] S. Nojiri and S. D. Odintsov, Phys. Rev. **D68**, 123512 (2003), hep-th/0307288.
 - [6] S. Nojiri and S. D. Odintsov, Phys. Lett. **B576**, 5 (2003), hep-th/0307071.
 - [7] V. Faraoni, Phys. Rev. **D72**, 124005 (2005), gr-qc/0511094.
 - [8] A. de la Cruz-Dombriz and A. Dobado, Phys. Rev. **D74**, 087501 (2006), gr-qc/0607118.
 - [9] N. J. Poplawski, Phys. Rev. **D74**, 084032 (2006), gr-qc/0607124.
 - [10] A. W. Brookfield, C. van de Bruck, and L. M. H. Hall, Phys. Rev. **D74**, 064028 (2006), hep-th/0608015.
 - [11] B. Li, K. C. Chan, and M. C. Chu (2006), astro-ph/0610794.
 - [12] T. P. Sotiriou and S. Liberati, Annals Phys. **322**, 935 (2007), gr-qc/0604006.
 - [13] T. P. Sotiriou, Phys. Lett. **B645**, 389 (2007), gr-qc/0611107.
 - [14] T. P. Sotiriou, Class. Quant. Grav. **23**, 5117 (2006), gr-qc/0604028.
 - [15] R. Bean, D. Bernat, L. Pogosian, A. Silvestri, and M. Trodden, Phys. Rev. **D75**, 064020 (2007), astro-ph/0611321.
 - [16] S. Baghram, M. Farhang, and S. Rahvar, Phys. Rev. **D75**, 044024 (2007), astro-ph/0701013.
 - [17] D. Bazeia, B. Carneiro da Cunha, R. Menezes, and A. Y. Petrov (2007), hep-th/0701106.
 - [18] B. Li and J. D. Barrow, Phys. Rev. **D75**, 084010 (2007), gr-qc/0701111.
 - [19] S. Bludman (2007), astro-ph/0702085.
 - [20] T. Rador (2007), hep-th/0702081.
 - [21] T. Rador, Phys. Rev. **D75**, 064033 (2007), hep-th/0701267.
 - [22] L. M. Sokolowski (2007), gr-qc/0702097.
 - [23] V. Faraoni, Phys. Rev. **D75**, 067302 (2007), gr-qc/0703044.
 - [24] V. Faraoni, Phys. Rev. **D74**, 104017 (2006), astro-ph/0610734.
 - [25] S. Nojiri and S. D. Odintsov, Gen. Rel. Grav. **36**, 1765 (2004), hep-th/0308176.
 - [26] P. Wang and X.-H. Meng, TSPU Vestnik **44N7**, 40 (2004), astro-ph/0406455.
 - [27] X.-H. Meng and P. Wang, Gen. Rel. Grav. **36**, 1947 (2004), gr-qc/0311019.
 - [28] M. C. B. Abdalla, S. Nojiri, and S. D. Odintsov, Class. Quant. Grav. **22**, L35 (2005), hep-th/0409177.
 - [29] G. Cognola, E. Elizalde, S. Nojiri, S. D. Odintsov, and S. Zerbini, JCAP **0502**, 010 (2005), hep-th/0501096.
 - [30] S. Capozziello, V. F. Cardone, and A. Troisi, Phys. Rev. **D71**, 043503 (2005), astro-ph/0501426.
 - [31] G. Allemandi, A. Borowiec, M. Francaviglia, and S. D. Odintsov, Phys. Rev. **D72**, 063505 (2005), gr-qc/0504057.
 - [32] T. Koivisto and H. Kurki-Suonio, Class. Quant. Grav. **23**, 2355 (2006), astro-ph/0509422.
 - [33] T. Clifton and J. D. Barrow, Phys. Rev. **D72**, 103005 (2005), gr-qc/0509059.
 - [34] O. Mena, J. Santiago, and J. Weller, Phys. Rev. Lett. **96**, 041103 (2006), astro-ph/0510453.
 - [35] M. Amarzguoui, O. Elgaroy, D. F. Mota, and T. Multamaki, Astron. Astrophys. **454**, 707 (2006), astro-ph/0510519.
 - [36] I. Brevik, Int. J. Mod. Phys. **D15**, 767 (2006), gr-qc/0601100.
 - [37] T. Koivisto, Phys. Rev. **D73**, 083517 (2006), astro-ph/0602031.
 - [38] S. E. Perez Bergliaffa, Phys. Lett. **B642**, 311 (2006), gr-qc/0608072.
 - [39] G. Cognola, M. Gastaldi, and S. Zerbini (2007), gr-qc/0701138.
 - [40] S. Capozziello and R. Garattini, Class. Quant. Grav. **24**, 1627 (2007), gr-qc/0702075.
 - [41] S. Nojiri and S. D. Odintsov, Phys. Rev. **D74**, 086005 (2006), hep-th/0608008.

- [42] S. Nojiri and S. D. Odintsov (2006), hep-th/0610164.
- [43] S. Capozziello, S. Nojiri, S. D. Odintsov, and A. Troisi, Phys. Lett. **B639**, 135 (2006), astro-ph/0604431.
- [44] S. Fay, S. Nesseris, and L. Perivolaropoulos (2007), gr-qc/0703006.
- [45] S. Fay, R. Tavakol, and S. Tsujikawa, Phys. Rev. **D75**, 063509 (2007), astro-ph/0701479.
- [46] S. Nojiri, S. D. Odintsov, and M. Sasaki, Phys. Rev. **D71**, 123509 (2005), hep-th/0504052.
- [47] M. Sami, A. Toporensky, P. V. Tretjakov, and S. Tsujikawa, Phys. Lett. **B619**, 193 (2005), hep-th/0504154.
- [48] G. Calcagni, S. Tsujikawa, and M. Sami, Class. Quant. Grav. **22**, 3977 (2005), hep-th/0505193.
- [49] S. Tsujikawa and M. Sami, JCAP **0701**, 006 (2007), hep-th/0608178.
- [50] Z.-K. Guo, N. Ohta, and S. Tsujikawa, Phys. Rev. **D75**, 023520 (2007), hep-th/0610336.
- [51] A. K. Sanyal, Phys. Lett. **B645**, 1 (2007), astro-ph/0608104.
- [52] B. M. Leith and I. P. Neupane (2007), hep-th/0702002.
- [53] B. M. N. Carter and I. P. Neupane, JCAP **0606**, 004 (2006), hep-th/0512262.
- [54] T. Koivisto and D. F. Mota, Phys. Rev. **D75**, 023518 (2007), hep-th/0609155.
- [55] T. Koivisto and D. F. Mota, Phys. Lett. **B644**, 104 (2007), astro-ph/0606078.
- [56] S. Nojiri, S. D. Odintsov, and M. Sami, Phys. Rev. **D74**, 046004 (2006), hep-th/0605039.
- [57] S. Nojiri and S. D. Odintsov (2006), hep-th/0611071.
- [58] G. Cognola, E. Elizalde, S. Nojiri, S. Odintsov, and S. Zerbini, Phys. Rev. **D75**, 086002 (2007), hep-th/0611198.
- [59] S. Nojiri and S. D. Odintsov, Phys. Lett. **B631**, 1 (2005), hep-th/0508049.
- [60] G. Cognola, E. Elizalde, S. Nojiri, S. D. Odintsov, and S. Zerbini, Phys. Rev. **D73**, 084007 (2006), hep-th/0601008.
- [61] Y.-S. Song, W. Hu, and I. Sawicki, Phys. Rev. **D75**, 044004 (2007), astro-ph/0610532.
- [62] S. Nojiri, S. D. Odintsov, and P. V. Tretyakov (2007), arXiv:0704.2520 [hep-th].
- [63] T. Multamaki and I. Vilja, Phys. Rev. **D73**, 024018 (2006), astro-ph/0506692.
- [64] R. P. Woodard (2006), astro-ph/0601672.
- [65] T. P. Sotiriou, Gen. Rel. Grav. **38**, 1407 (2006), gr-qc/0507027.
- [66] J. A. R. Cembranos, Phys. Rev. **D73**, 064029 (2006), gr-qc/0507039.
- [67] G. Allemandi, M. Francaviglia, M. L. Ruggiero, and A. Tartaglia, Gen. Rel. Grav. **37**, 1891 (2005), gr-qc/0506123.
- [68] M. L. Ruggiero and L. Iorio, JCAP **0701**, 010 (2007), gr-qc/0607093.
- [69] T. P. Sotiriou and E. Barausse, Phys. Rev. **D75**, 084007 (2007), gr-qc/0612065.
- [70] C.-G. Shao, R.-G. Cai, B. Wang, and R.-K. Su, Phys. Lett. **B633**, 164 (2006), gr-qc/0511034.
- [71] A. J. Bustelo and D. E. Barraco, Class. Quant. Grav. **24**, 2333 (2007), gr-qc/0611149.
- [72] G. J. Olmo, Phys. Rev. **D75**, 023511 (2007), gr-qc/0612047.
- [73] P.-J. Zhang (2007), astro-ph/0701662.
- [74] K. Kainulainen, J. Piilonen, V. Reijonen, and D. Sunhede (2007), arXiv:0704.2729 [gr-qc].
- [75] T. Chiba, Phys. Lett. **B575**, 1 (2003), astro-ph/0307338.
- [76] A. L. Erickcek, T. L. Smith, and M. Kamionkowski, Phys. Rev. **D74**, 121501 (2006), astro-ph/0610483.
- [77] T. Chiba, T. L. Smith, and A. L. Erickcek (2006), astro-ph/0611867.
- [78] J. Khoury and A. Weltman, Phys. Rev. **D69**, 044026 (2004), astro-ph/0309411.
- [79] I. Navarro and K. Van Acoleyen (2006), gr-qc/0611127.
- [80] T. Faulkner, M. Tegmark, E. F. Bunn, and Y. Mao (2006), astro-ph/0612569.
- [81] L. Amendola, D. Polarski, and S. Tsujikawa (2006), astro-ph/0603703.
- [82] I. Sawicki and W. Hu, Phys. Rev. D in press, astro (2007), astro-ph/0702278.
- [83] P. Zhang, Phys. Rev. **D73**, 123504 (2006), astro-ph/0511218.
- [84] A. A. Starobinsky, Phys. Lett. **B91**, 99 (1980).
- [85] T. Faulkner, M. Tegmark, E. F. Bunn, and Y. Mao (2006), astro-ph/0612569.
- [86] A. Vikman, Phys. Rev. **D71**, 023515 (2005), astro-ph/0407107.
- [87] W. Hu, Phys. Rev. D **71**, 047301 (2005), astro-ph/0410680.
- [88] Z.-K. Guo, Y.-S. Piao, X.-M. Zhang, and Y.-Z. Zhang, Phys. Lett. **B608**, 177 (2005), astro-ph/0410654.
- [89] L. Amendola and S. Tsujikawa (2007), arXiv:0705.0396 [astro-ph].
- [90] A. D. Dolgov and M. Kawasaki, Phys. Lett. **B573**, 1 (2003), astro-ph/0307285.
- [91] M. D. Seifert (2007), gr-qc/0703060.
- [92] J. N. Bahcall, A. M. Serenelli, and S. Basu, Astrophys. J. Lett. **621**, L85 (2005), arXiv:astro-ph/0412440.
- [93] J. E. Vernazza, E. H. Avrett, and R. Loeser, Astrophys. J. Supp. **45**, 635 (1981).
- [94] E. C. Sittler, Jr. and M. Guhathakurta, Astrophys. J. **523**, 812 (1999).
- [95] C. M. Will, Living Reviews in Relativity **9** (2006), URL <http://www.livingreviews.org/lrr-2006-3>.
- [96] A. Klypin, H. Zhao, and R. S. Somerville, Astrophys. J. **573**, 597 (2002), astro-ph/0110390.